JOURNAL OF PROPULSION AND POWER
Vol. 11, No. 6, November–December 1995

Effect of Dilution Air on the Scalar Flowfield at Combustor Sector Exit

A. Gulati,* A. Tolpadi,† and G. VanDeusen†
General Electric Corporate R&D Center, Schenectady, New York 12301
and
D. Burrus‡
General Electric Aircraft Engines, Cincinnati, Ohio 45215-6301

Spontaneous Raman diagnostics are applied to the exit plane of a full-scale 10-cup double-annular research combustor sector to obtain the mean and rms of temperature and mole fractions of major species for comparison with predictions of the code CONCERT-3D for the same geometry and operating conditions. CONCERT-3D has been developed and used extensively in the past and represents a fully elliptic three-dimensional computational fluid dynamics code to predict flowfields in practical full-scale combustors. The theory/data comparison is encouraging. The mean and rms temperature profiles and mean profiles of the major species are predicted quite well by the model. Dilution air is shown to have a significant impact on the mean and rms temperature profiles at the sector exit. The mean temperature profile is forced inbound by the outer dilution air, whereas the inner dilution air forces the temperature profile to be center-peaked with lower peak values. The rms turbulence fluctuation levels are generally increased by the dilution air. The effect on profiles of major species is similar. CONCERT-3D predicts these trends well. Overall, larger values of rms fluctuations are measured than predicted by the model. Possible reasons for these and other differences are discussed.

Introduction

UNDERSTANDING and predicting the role of dilution air in advanced aircraft gas-turbine combustor design is becoming increasingly important as combustors are operated at increased stoichiometric values in an attempt to achieve higher engine efficiencies. Dilution air is conventionally introduced through rows of large holes in the outer and inner liners within the region between the main combustion zone (primary zone) and the combustor exit. The primary role of dilution air is to lower the bulk exit temperature to levels permissible by turbine material considerations, to shape the temperature profile, and to obtain an acceptable pattern factor at the combustor exit. In general, there is more than one row of dilution air (primary, secondary, and tertiary). Because of the proximity of secondary and tertiary dilution jets to the combustor exit and the turbulent mixing of the jets, large fluctuations in temperature and mixture fraction values are suspected to be present at the exit plane of the combustor. A recent experimental study of a combustor sector reported significant scalar fluctuations to be indeed present at the exit of such a combustor.[1] Such fluctuations are believed to be responsible, in part, for the phenomena of hot streaks at the combustor exit. Hot streaks are undesirable, they represent losses in combustor efficiency, contribute to NO_x emissions, and can cause damage to turbine hardware. It is therefore important to understand and quantify the effect of dilution air on the exit scalar flowfield. In this article we present results of a combined experimental/modeling effort to better understand its role.

The research vehicle used in this study is a double-annular 10-cup combustor sector representing a 75-deg section of a full annular combustor. Henceforth, this combustor will be referred to as a five-cup sector, by which it is meant that there are five cups in the inner dome and five in the outer dome, thus making a total of 10 cups. Experimental data are obtained at the exit of the five-cup sector by applying the technique of spontaneous Raman/Rayleigh scattering. The experimental results are compared with model predictions based upon CONCERT-3D code simulations. CONCERT-3D is a fully elliptic three-dimensional body-fitted computational fluid dynamics code developed extensively[2–6] over the years that combines reasonable combustion models with good numerical procedures to yield a comprehensive modeling capability for single- and two-phase flow predictions in practical gas-turbine combustor geometries. The code is applied to the combustor sector at the same operating conditions for which experimental data has been obtained. The role of dilution air is examined by studying three different hardware configurations with holes of secondary dilution air in the outer and inner liners of the combustor sector closed/closed, open/closed, or open/open, respectively.

Experimental Setup

The joint Raman/Rayleigh diagnostic system used in this study is similar to that used in the past,[7–9] with some modifications[1] to allow measurements in a practical combustor. In brief, the Raman system consists of a Candela LFDL-20 flashlamp pumped dye laser that provides pulses of ~1 J in ~2 μs, within a 0.2-nm bandpass at 488.0 nm at 10 Hz. The laser beam is approximately 1 cm in diameter and is focused by a 200-mm lens forming the probe volume. The Raman scattered light is collected at right angles by an achromatic 250-mm $f/2$ lens and is then collimated and refocused onto the entrance slit of a 3/4-m Spex polychrometer following a $\times 3$ magnification. The probe volume dimensions are approximately 0.3 mm $\times$ 0.3 mm $\times$ 0.6 mm. The collected light is then dispersed for detection by numerous RCA 4526 photomultiplier tubes located at appropriate locations in the exit plane (Fig. 1) for detecting anti-Stokes Raman scattering from nitrogen, Stokes vibrational Raman scattering from N_2, O_2, H_2, H_2O, CO, CO_2, and unburnt hydrocarbons (C-H

Presented as Paper 94-0221 at the AIAA 32nd Aerospace Sciences Meeting, Reno, NV, Jan. 10–13, 1994; received Jan. 25, 1994; revision received Feb. 16, 1995; accepted for publication Feb. 18, 1995.

*Mechanical Engineer. Member AIAA.
†Mechanical Engineer.
‡Staff Engineer. Member AIAA.

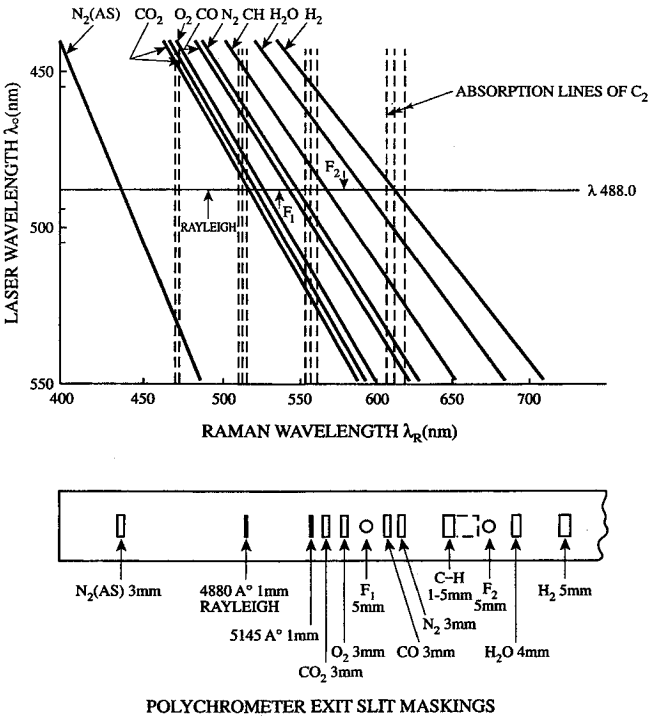

Fig. 1 Schematic location of Raman vibrational bands and polychrometer exit slit maskings for major species.

bond) and Rayleigh scattering. The differential voltages corresponding to the Raman signal minus the background are collected using custom-designed simultaneous sample and hold circuitry and are recorded for postprocessing using an IBM-AT based data acquisition system.

The Raman system has been modified to correct for laser-induced fluorescence interference by the addition of two photomultiplier tubes termed "F_1" and "F_2" to monitor laser-induced fluorescence at the exit plane of the polychrometer in Raman-free regions of the spectra, as shown in Fig. 1 and described in detail elsewhere.[1,10–12] For the present application, a minimal amount of interference in the Raman signals was observed since the combustor operates in a partially premixed mode.[1] All of the data have been corrected for laser-induced fluorescence on a shot-to-shot basis. The data is processed as follows: the Raman signals are first corrected for electrical noise and the mole fractions of major species obtained using calibration factors developed with 100% pure gases and well-calibrated gas mixtures. The fluorescence correction factors to account for laser-induced fluorescence, if any, are then applied. The temperature is obtained using the following iterative procedure[1,13]: the initial value of temperature is guessed, based upon which mole fractions for all major species are calculated using the equation of state, their measured vibrational intensities, and high-temperature correction factors. The process is repeated until the sum of mole fractions is unity. Convergence is typically obtained in one or two iterations. Earlier work[1,7–9] had shown this method to yield the most accurate results in similar applications.

The five-cup double-annular research combustor sector used in this study represents a 75-deg section of a full annular combustor. The sector provides an exact simulation of the general flow features while requiring only a fraction of the airflow needed for the full combustor. One drawback to the sector is the potential impact of sector sidewalls. The combustor sector represents a short-length dual-annular dome design. Each mixer cup features a two-stage counter-rotating radial inflow-type swirler package with a simplex-type pressure atomizing injector located centrally within the first swirler stage. Combustor liner cooling is achieved using a multihole approach. The combustor also employs a rather

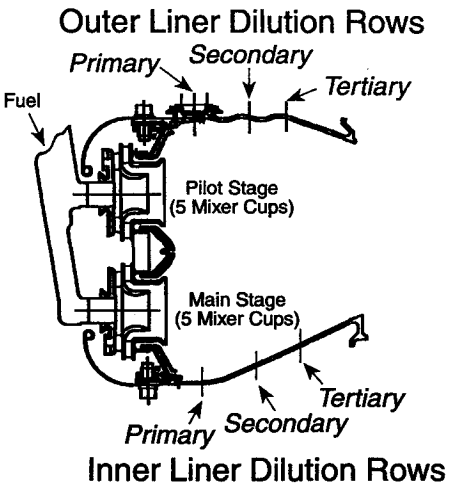

Fig. 2 Schematic of five-cup double annular research combustor sector.

complex pattern of liner and centerbody dilution. For the outer liner, there are three rows of dilution holes arranged in the following pattern; row 1 (closest to the primary zone–primary dilution) consists of one hole per cup section located in-line with the cup centerline; row 2 (located further downstream–secondary dilution) consists of three holes per cup section located at ±2.5 deg and ±7.5 deg relative to the cup centerline; row 3 (closest to sector exit–tertiary dilution) consists of three holes per cup section located in-line with the cup centerline and ±5.0 deg relative to the cup centerline. Note that for row 2, the holes located at ±7.5 deg actually lie along the boundary between adjacent cups. As such, only half of each hole is considered to be within the cup section. For the inner liner also there are three rows of dilution holes arranged in a similar pattern, the primary row consists of one hole per cup section located at ±7.5 deg relative to the cup centerline; the secondary row consists of two holes per cup section located in-line with the cup centerline and at ±7.5 deg relative to the cup centerline; and the tertiary row consists of two holes per cup section located at ±3.75 deg relative to the cup centerline. Figure 2 provides a schematic of the sector and the dilution rows. The following three sector configurations were examined in this study: configuration no. 1 in which the secondary dilution row holes on both the outer and inner liners were blocked off (henceforth, referred to as OC/IC for outer closed/inner closed), configuration no. 2 with the outer liner secondary dilution row holes opened and the inner closed (OO/IC), and configuration no. 3 in which both the outer and inner liner secondary dilution rows were opened (OO/IO). The sector exit is 100 mm wide with the inner annuli of radius 180 mm and the outer annuli of radius 280 mm approximately.

Governing Equations and the Numerical Approach

The governing equations represent the conservation of mass and momentum in the three coordinate directions. Turbulence is modeled using the standard k-ε turbulence model. The combustion model utilizes a conserved scalar variable for the fuel mixture fraction with assumed probability density function (PDF) and a fast chemistry approach for the turbulence/chemistry interaction.[2] A conservation equation is also written for the fluctuation in the mixture fraction.[14] This fluctuation is modeled as the variance of the mixture fraction. The equilibrium density for the fuel is initially obtained as a function of the mixture fraction. Assuming a beta PDF, and convoluting this equilibrium distribution with the PDF, a look-up table is generated that contains the density as a function of the mixture fraction and its variance.[2] Thus, based upon the computed values of the mixture fraction and its variance, the density field is obtained from this table and is used in all

of the equations that are being solved. Using a coordinate transformation, the governing equations are transformed from, in general, an arbitrarily shaped physical domain to a rectangular parallelepiped. The equations are solved in this boundary-fitted coordinate system using the SIMPLE pressure correction algorithm.[15] The governing equations, their discretization, and the numerical algorithm have been described in detail elsewhere.[3-5]

The temperature field, the variance of the temperature (from which the rms temperature is calculated), and the distribution of the mole fractions of species within the combustor are all obtained as a postprocessing step. In the same manner as the density, the equilibrium temperature and species mole fractions are initially obtained as a function of the mixture fraction. These equilibrium distributions are convoluted with the PDF to yield a second look-up table that contains the temperature, its variance, and the species mole fractions as a function of the mixture fraction and its variance. The distribution of all these quantities within the combustor are then obtained from this second look-up table using bilinear interpolation based upon calculated values of the mixture fraction and its variance.

Application of CONCERT-3D to Sector

A single-cup section of the combustor sector was first modeled within the structured body-fitted grid. It was assumed that the single cup behaved exactly the same as its adjacent neighbors, allowing the use of periodic boundary conditions at the interfaces and a reduced manageable grid. The single-cup section represents the center cups of the five-cup sector. A common grid was generated for use with all three combustor configurations. The CONCERT-3D grid generator allows the inclusion of circular features into the grid surfaces to represent liner dilution holes and inlet plane swirler/mixer discharge features. The single-cup section was modeled using a grid mesh of 45 × 49 × 25 (total = 55,125) points. This level of grid density allows for acceptable run times and costs and provides exit pattern factor solutions with sufficient accuracy.[2-5] For the three configurations the secondary row dilution features were activated/deactivated as necessary to replicate the test configurations. Figure 3 presents an isometric view of the single-cup section grid mesh. The CONCERT-3D model extended only to the exit plane of the combustor. The effects of the entrainment of room air at the combustor exit are therefore not represented. To explore the impact of the sidewalls a CONCERT-3D model of the entire five-cup sector was also generated. This grid mesh replicated the exact single-cup grid mesh five times over. The resulting grid consists of 45 × 49 × 131 (288,855) points. This approach eliminated any grid density differences between the two models. Figure 4 presents an isometric view of the generated grid mesh. For the five-cup section model, wall boundary conditions were imposed along the two tangential boundaries to represent the presence of the test rig sidewalls.

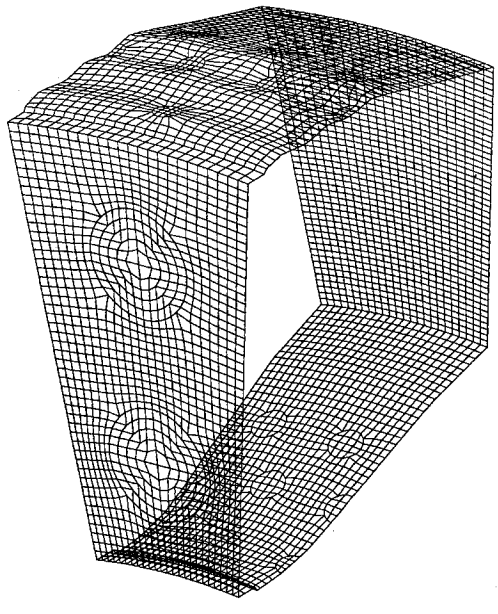

Fig. 3 Isometric three-dimensional view of computational grid for single-cup section modeling.

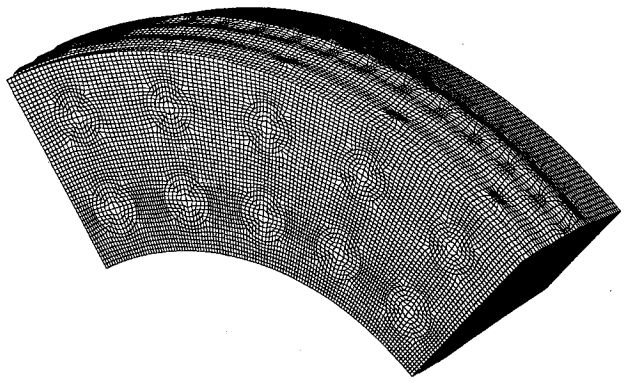

Fig. 4 Isometric three-dimensional view of computational grid for full five-cup sector modeling.

Boundary conditions that need to be specified for the model calculations are the inlet air temperature, pressure, total airflow, total fuel flow, airflow distribution for the array of combustor air injection features, fuel flow distribution to each inlet swirl cup mixer/injector, and the velocity and fuel distribution characteristics discharging from each swirl cup mixer/injector. The airflow distribution boundary conditions are based upon a measured airflow calibration test. The swirl cup mixer/injector discharge velocity characteristics are based upon laser velocimetry data used earlier to qualify a CONCERT-2D axisymmetric model of the cup. Gaseous fuel is assumed in all modeling even though liquid fuel is used in the experiment, which is reasonable since the elevated temperature of 600 K for combustor sector operation should result in short droplet lifetimes given the excellent atomization characteristics of the mixer/injector used in this combustor. In the application of practical combustors at low power conditions such as at idle, the droplet lifetimes can be significant and will have to be included in the analysis.[5] Internal heat transfer effects, including convection to the linear walls and radiation effects, are not modeled in these calculations. Each single-cup section model was run for 1500 iterations producing acceptably converged solutions. The five-cup sector model was run only for test configuration no. 3 (OO/IO). This larger model required a total of 4500 iterations to achieve similar levels of convergence. Convergence is based upon levels of the residuals for the mass, momentum, and kinetic energy equations and on the overall level of kinetic energy in the calculation.

Application of Raman to Sector

The Raman system consisting of the laser and the receiving optics is mounted on a three-dimensional traversing table. The optics of the Raman system are modified such that the collecting lens is at an angle of 60 deg to the main flow axis to allow closer optical access. The sector is mounted in a large plenum with a modified face plate that allows optical access to within 12.5 mm of the sector exit with the modified Raman system. All the Raman data is obtained at this axial plane. Numerous radial profiles spanning the sector exit are obtained for each configuration. Figure 5 shows a schematic of the experimental setup. All of the cups of the sector are fueled. Liquid fuel (kerosene) is used. The sector is operated with preheated air of up to 600 K. Flow capabilities allow operation

Table 1 Table listing operating conditions for the three configurations

Configuration	P combustor, mm-Hg	T inlet, K	Airflow, kg/s	Fuel outer annulus, kg/s	Fuel inner annulus, kg/s	Fuel outer annulus, %	Total fuel, kg/s	Overall equivalence ratio
OC/IC	24.70	555	0.600	0.0049	0.0065	43.0	0.0114	0.29
OO/IC	24.70	555	0.684	0.0054	0.0074	42.4	0.0128	0.29
OO/OO	24.70	555	0.741	0.0059	0.0077	43.3	0.0136	0.29

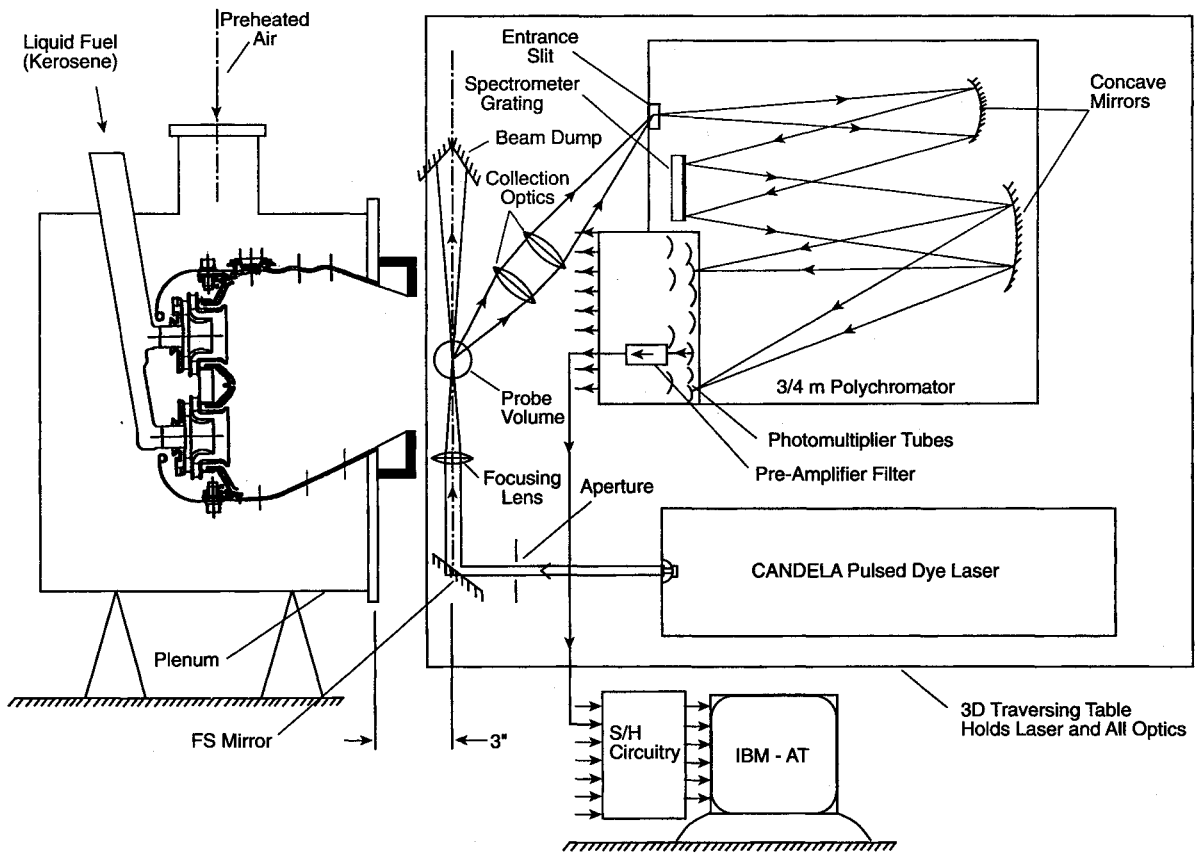

Fig. 5 Schematic of combustor sector and Raman setup.

over a wide range of air flow rates (up to 2 kg/s) and equivalence ratios (up to stoichiometric).

Results

Comparison of Model Predictions with Raman Data

Table 1 lists the operating conditions for the three configurations. In all cases the air pressure drop across the combustor was maintained constant at 24.7 mm of Hg, the combustor inlet temperature at 555 K, and the overall equivalence 0.29 with 43% of fuel going to the outer annulus. This was done to assure dynamics-free operation since the combustor was found to exhibit low-frequency rumble with matched fuel flow rate (50% each annuli) at these conditions. The Raman data presented here are in terms of derived statistical quantities (mean and rms) based upon 200 data points at every location. The CONCERT-3D modeling results are based upon single-cup section model.

Figures 6–8 show comparisons of the predicted mean and rms temperature profiles and mean profiles of mole fraction of major species with Raman data at the centerline of the sector for the OC/IC configuration. The ordinate (y axis) in all figures is the percent height with zero representing the bottom of the sector exit and 100% corresponding to the top of the sector exit. The thermocouple data shown in Fig. 6 for comparative purposes has been obtained with a type-B double-sheathed thermocouple located 12.5 mm further downstream of the Raman probe volume. Figure 6 shows that the mean temperature profile at the centerline is predicted well by the model. The profile is inner-peaked for this configuration with the peak value closely matching the measured thermocouple data. The trends for the thermocouple data and the Raman data agree. The thermocouple data have been corrected for radiation losses. The double-sheath arrangement used to minimize radiation loss makes the estimation of convective losses extremely difficult. The Raman data for temperature involves an estimated uncertainty of ± 70 K on a shot-to-shot basis and ± 20 K for the mean value. The sharp drop in the mean temperature profile at the edges in the experimental data is probably due to entrainment of room air beyond the sector exit and is not taken into account in the model. Both the CONCERT-3D and the measured temperature profiles show an almost linear increase toward the peak from the outer edge of the sector exit.

Figure 7 shows the comparison of rms temperature (normalized by local mean) predictions with measured Raman data. The Raman data shown are for true rms values. True rms are estimated to be 1–2% lower than the measured values, depending upon the location due to the estimated[1] shot-to-shot rms Raman temperature variation of up to 5%. The comparison of the rms temperature profile is encouraging. The shape of the profile with a peak in the center and sharp rise at the edges is predicted well. CONCERT-3D, however, consistently predicts lower rms values than measured. A pos-

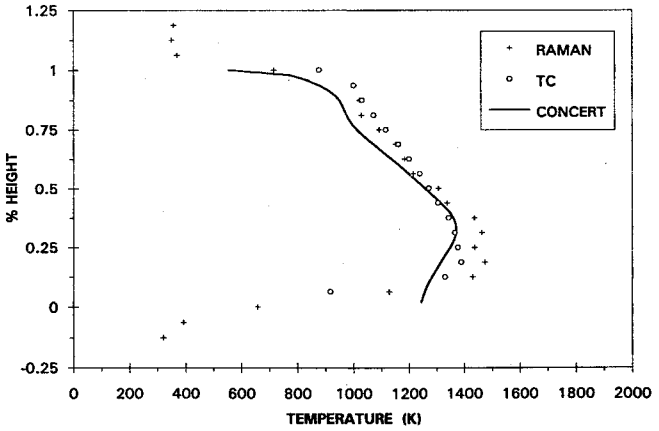

Fig. 6 Comparison of mean temperature profile at the centerline of the sector exit obtained with Raman diagnostics and thermocouple data with CONCERT-3D model predictions for OC/IC configuration (Figs. 6–8). Operating conditions listed in Table 1 for Figs. 6–12.

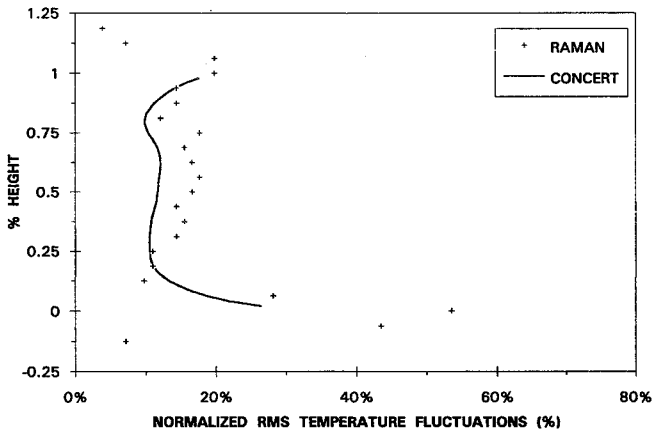

Fig. 7 Centerline profiles of normalized rms temperature fluctuations.

sible reason could be the effect of the turbulence model and the constants used in the code predictions. It is well known[14] that the standard k-ε turbulence model has certain deficiencies when applied to highly swirling flows, particularly in the prediction of mixing levels that can be lower such as those observed here. Also, the combustion model used in this code assumes fast chemistry and does not account for possible finite rate chemistry effects that may contribute to the differences. The data presented here are based on an assumed value of 0.25 for the turbulent Schmidt number in the equations for the mixture fraction and its variance. Code predictions of turbulence levels are sensitive to the value of this constant. The value of the Schmidt number used here is consistent with other applications of this model.[5]

A comparison of measured centerline profiles of major species with predicted values is shown in Fig. 8. The profiles for nitrogen and oxygen are predicted very well. Raman measurements for these major species are estimated to involve an estimated uncertainty of $\pm 1\%$ for mean mole fraction values. The profile for oxygen shows a minimum in the bottom half of the annuli corresponding to the peak in temperature as expected. The other major species corresponding to water and carbon dioxide are shown in Fig. 8b. The profile for water is inner-peaked for both the measured and the predicted quantities, as was the case with the temperature profile, and the data agrees well. For carbon dioxide, the trends are predicted correct, but the data does not peak to as high values as predicted. This is believed to be due to inaccuracies in measuring carbon-dioxide due to the complexity of the molecule, its close

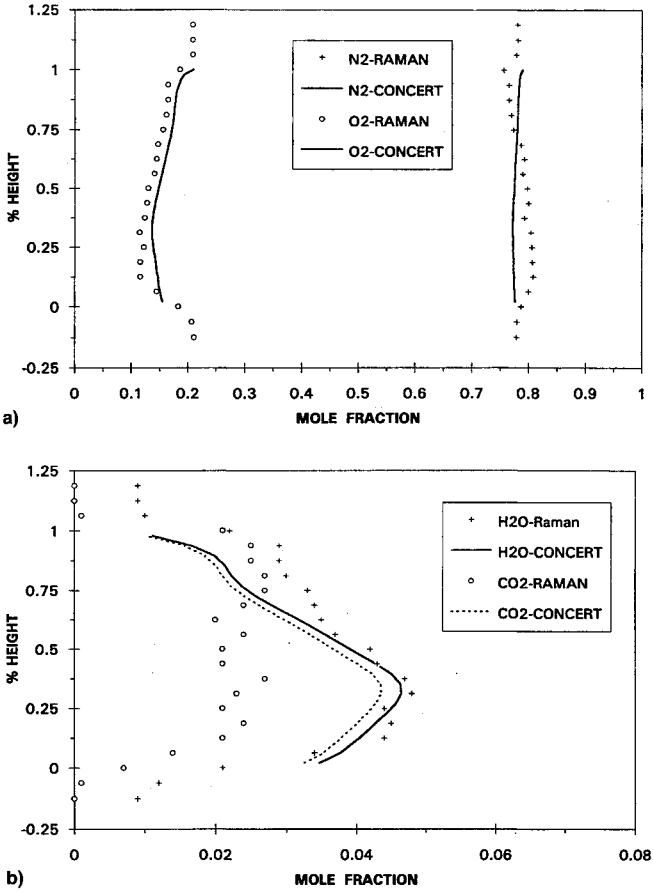

Fig. 8 Centerline profiles of mean mole fraction of major species: a) N_2 and O_2 and b) H_2O and CO_2.

proximity to oxygen, and the fact that only a small fraction of the Raman fundamental vibrational band overlaps the exit slit masking provided for carbon dioxide. Thus, the Raman signals for carbon dioxide are inherently low and its high-temperature correction factors difficult to estimate. The error bars for Raman measurements of water and carbon dioxide are estimated to be $\pm 10\%$ and $\pm 50\%$ of the mean, respectively. This is consistent with reported accuracies for Raman measurements in other similar studies.[9,11] The data for the remaining species, i.e., hydrogen, carbon monoxide, and unburned hydrocarbons are not shown because the predicted and measured values are both negligible (less than 1%). This also suggests that the flame front does not extend beyond the sector exit as confirmed by visual observations. Random streaks are, however, observed intermittently.

Effect of Dilution Air

Figure 9 shows the effect of dilution air on the centerline mean temperature profile. The trend is predicted correctly. The predicted profiles and the measured data show that as the outer row of dilution air is opened, the profile becomes more inner-peaked, i.e., the jets appear to push the combustion zone more toward the inner liner and the peak value increases. The opening of the inner row of dilution air (OO/IO) has an opposite and more dramatic effect, probably because the jets are closer to the combustion zone as evidenced by the inner-peaked profile. The inner dilution air shifts the peak of the temperature profile back towards the center and the peak value is lowered. The drop in the peak value suggests that the inner dilution air penetrates the combustion zone and leads to enhanced mixing and cooling of the combustion products. The overall effect of outer and inner dilution (OO/IO) is to thus make the temperature profile center-peaked with a lower peak value. Figure 9 clearly shows the dramatic impact

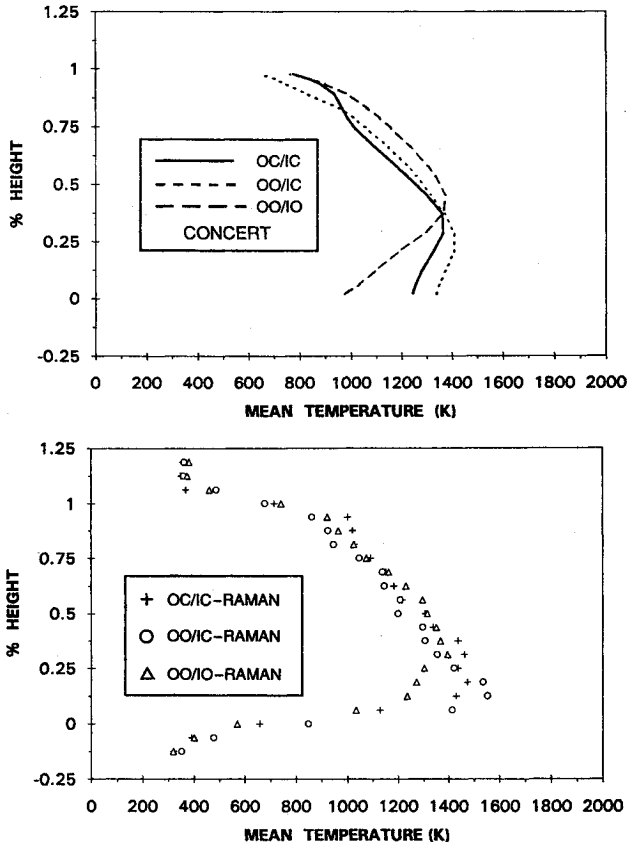

Fig. 9 Effect of dilution air on mean temperature.

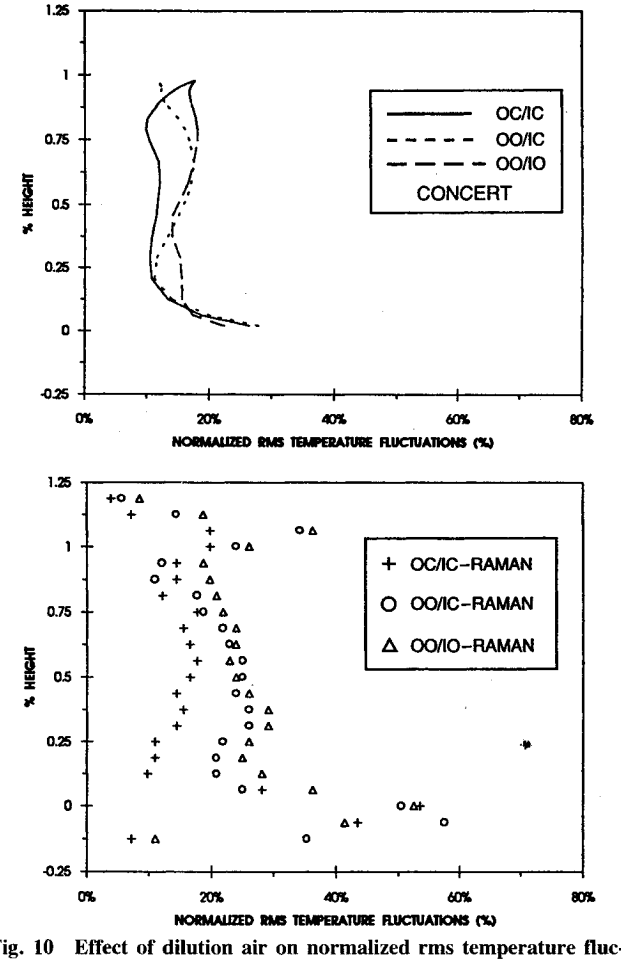

Fig. 10 Effect of dilution air on normalized rms temperature fluctuations.

of dilution air on the exit-temperature profile and its role in obtaining the desired exit pattern factor. The effect of dilution air on normalized rms temperature profiles at sector exit is shown in Fig. 10. The trends are predicted well, but the measured values are consistently larger than predicted as discussed earlier. There are other differences. The outer dilution air is predicted to increase the rms turbulence level throughout the exit profile with a more dramatic increase in the upper half of exit profile, whereas the measured data show a larger increase in turbulence levels in the bottom half of the temperature profile. The effect of inner dilution air is, however, predicted correctly and is seen to result in overall enhanced turbulence levels at the exit plane with a marked increase in the bottom half of the sector exit.

The effect of dilution air on the mean temperature profile at a circumferential location midway between adjacent cups is shown in Fig. 11. Similar effect is observed at this location, as at the centerline. The predicted and measured profiles show similar trends, i.e., that the outer dilution air causes a slight inbound shift in the peak of the temperature profile and increases it slightly, whereas the inner dilution air decreases the peak and results in a more center-peaked (in this case slightly outboard) temperature profile. At this location, however, dilution air has less impact on the temperature profile.

The previous data show that the effect of dilution air is dependent upon the circumferential location in the exit plane. In order to obtain an estimate of the effect of dilution air on the overall sector exit temperature pattern the predicted and measured values of the average and maximum temperature at the sector exit plane are presented in Fig. 12 for the three configurations. For the CONCERT-3D predictions, the solution has been circumferentially averaged through all of the angular locations (over the single-cup section) to yield the

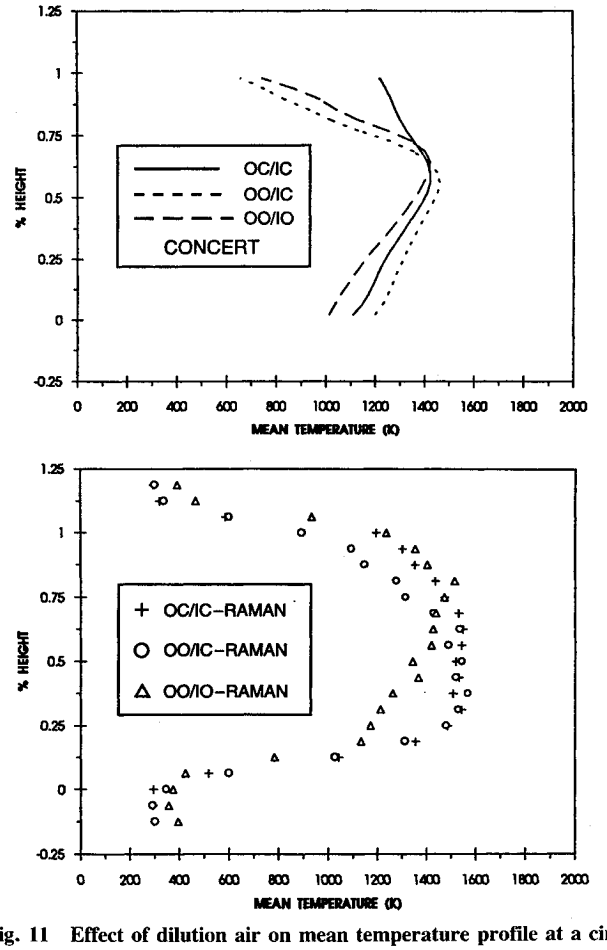

Fig. 11 Effect of dilution air on mean temperature profile at a circumferential location midway between two adjacent cups.

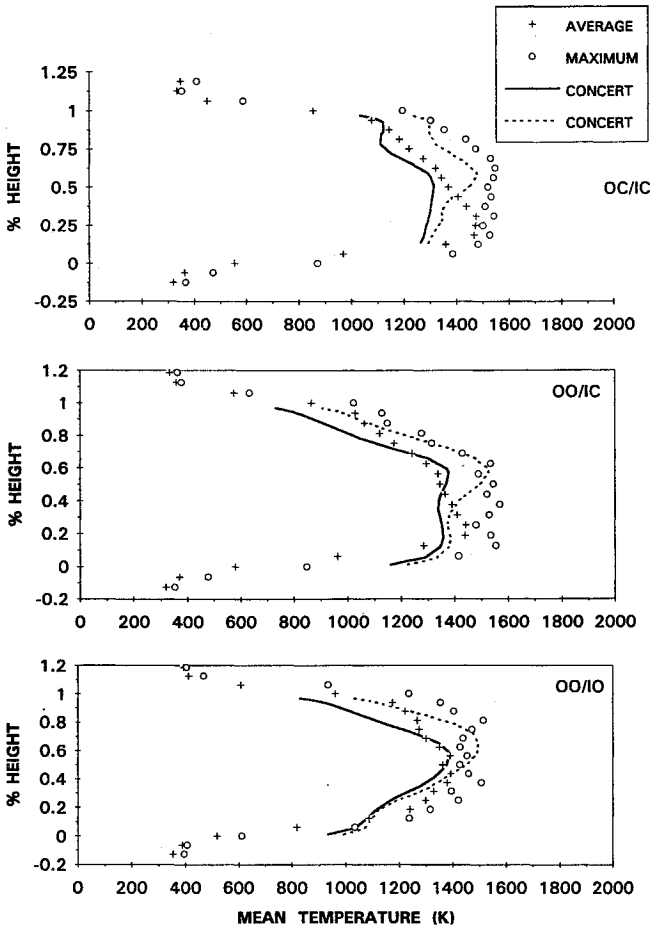

Fig. 12 Effect of dilution air on radial profiles of average and maximum temperature across one-cup (center-cup) section of the five-cup sector.

mean radial profile. The Raman data profiles are based upon the average and maximum of the three radial profiles obtained at the exit plane for all configurations. These profiles were obtained in-line with the center cup, midway between two adjacent cups, and in-line with the adjacent cup. Encouraging comparison is obtained for both the average and maximum values. As observed earlier, the outer dilution air results in more inner-peaked profile, whereas the combination of outer and inner dilution air results in a more center-peaked profile. The profile of the maximum temperature for the OO/IO configuration shows a double peak in the data. This is not clearly understood at present, but is believed to be due to cup-to-cup variations in the temperature field, probably due to cup-to-cup differences in physical hardware and inlet flow variations. Temperature rake data obtained in the past at the exit plane of full annulus combustor tests have shown similar significant circumferential variation in radial temperature profiles, which has been attributed to cup-to-cup variations in practical hardware.[16] To determine if the cup-to-cup variations could be a result of sidewalls and assumed periodic boundary conditions, a detailed CONCERT-3D calculation was done for the full five-cup sector for the OO/IO configuration using the grid shown in Fig. 4. The results (not presented here) showed a negligible effect of sidewalls and periodic boundary conditions on predictions in the center region of the sector. This shows that the single-cup section model is indeed representative of the center-cup region of the full five-cup sector.

Conclusions

1) The Raman system has been successfully applied to the exit plane of a full-scale five-cup double-annular combustor sector to obtain temperature and scalar flowfield measurements with liquid fuel (kerosene) and a good quality database has been established for direct comparison and qualification of CONCERT 3-D and other computational models.

2) The theory/data comparison looks encouraging and shows that mean and rms temperature profiles and mean profiles of major species are predicted well by the model. The centerline temperature profile is inner-peaked with both outer and inner dilution rows blocked (OC/IC configuration). The rms temperature values are underpredicted. The mean major species profiles follow a trend similar to mean temperature and the data are predicted well. Potential reasons for some differences have been noted. The greatest uncertainties in Raman measurements lie in the measurement of carbon dioxide. In terms of modeling the largest uncertainties are involved in the predictions of the turbulence levels. The role of turbulent Schmidt number, grid size, and the turbulence models used should be re-examined to improve predictive capabilities of the model. A more demanding comparison such as in the vicinity of swirl cup regions is required to further qualify the model and the Raman diagnostics system.

3) Dilution air has a significant effect on the mean and rms temperature profiles at the combustor exit. The outer dilution air forces the combustion zone further inward and results in slightly higher values of temperature (peak) there, whereas the inner dilution air causes an opposite trend and in combination with outer dilution results in a more center-peaked temperature profile with a reduced peak. Both of these trends are predicted well by the model. The model consistently underpredicts the level of turbulence fluctuations at the exit, although the trend of increased turbulence with dilution air is predicted correctly.

4) The impact of dilution air varies with circumferential location. The model again predicts the trends correctly. The model is, however, unable to account for cup-to-cup flowfield variations observed in the data. Comparison of single-cup section modeling results with full five-cup sector modeling shows that the single cup periodic section model is fairly representative of the center region of the full five-cup sector. Overall, the results show that dilution air can be used to tailor the flowfield at the sector exit and that CONCERT-3D represents a good tool to optimize combustor exit pattern factor via dilution air.

Acknowledgments

The technical assistance of Frank Haller is gratefully acknowledged. The authors are also grateful to Will Dodds and Ramani Mani for providing financial support and encouragement.

References

[1]Gulati, A., "Raman Measurements at the Exit of a Combustor Sector," *Journal of Propulsion and Power*, Vol. 10, No. 2, 1994, pp. 169–175.

[2]Shyy, W., Correa, S. M., and Braaten, M. E., "Computation of Flow in a Gas Turbine Combustor," *Combustion Science and Technology*, Vol. 58, 1988, pp. 97–117.

[3]Shyy, W., Tong, S. S., and Correa, S. M., "Numerical Recirculating Flow Calculation Using a Body-Fitted Coordinate System," *Numerical Heat Transfer*, Vol. 8, 1985, pp. 99–113.

[4]Tolpadi, A. K., and Braaten, M. E., "Study of Branched Turboprop Inlet Ducts Using a Multiple Block Grid Calculation Procedure," *Journal of Fluids Engineering*, Vol. 114, No. 3, 1992, pp. 379–385.

[5]Tolpadi, A. K., "Calculation of Two-Phase Flow in Gas Turbine Combustors," *Journal of Engineering for Gas Turbines and Power* (to be published).

[6]Shyy, W., and Braaten, M. E., "A Numerical Study of Flow in a Gas Turbine Combustor," AIAA Paper 87-2132, 1987.

[7]Gulati, A., and Correa, S. M., "Raman/LV Measurements and Modeling in a $CO/H_2/N_2$ Flame at High Reynolds Number," *Archi-*

vum Combustionis, Vol. 10, Nos. 1–4, 1990, pp. 17–39.

[8]Correa, S. M., and Gulati, A., "Measurements and Modeling of a Bluff Body Stabilized Flame," *Combustion and Flame*, Vol. 89, No. 2, 1992, pp. 195–213.

[9]Correa, S. M., Gulati, A., and Pope, S. B., "Raman Measurements and Joint PDF Modeling of a Non-Premixed Bluff Body-Stabilized Methane Flame," *25th Symposium (International) on Combustion* (Irvine, CA), The Combustion Inst., Pittsburgh, PA, 1994.

[10]Masri, A. R., Bilger, R. W., and Dibble, R. W., "Fluorescence Interference with Raman Measurements in Nonpremixed Flames of Methane," *Combustion and Flame*, Vol. 68, 1987, pp. 109–119.

[11]Dibble, R. W., Masri, A. R., and Bilger, R. W., "The Spontaneous Raman Scattering Technique Applied to Non-premixed Flames of Methane," *Combustion and Flame*, Vol. 67, 1987, pp. 189–206.

[12]Dibble, R. W., Starner, S. H., Masri, A. R., and Barlow, R. S., "An Improved Method of Data Acquisition and Reduction of Laser Raman-Rayleigh Scattering from Multispecies," *Applied Physics B, Special Issue on Combustion Diagnostics*, 1990, pp. 1727–1731.

[13]Drake, M. C., Lapp, M., and Penney, C. M., "Use of the Vibrational Raman Effect for Gas Temperature Measurements," *Temperature Its Measurement and Control in Science and Industry*, edited by J. F. Schooley, Vol. 5, Pt. 1, American Institute of Physics, New York, 1982, pp. 631–638.

[14]Jones, W. P., and Whitelaw, J. H., "Calculation Methods for Reacting Turbulent Flows: A Review," *Combustion and Flame*, Vol. 48, 1982, pp. 1–26.

[15]Patankar, S. V., *Numerical Heat Transfer and Fluid Flow*, McGraw–Hill, New York, 1980.

[16]Burrus, D. L., Chahrour, C. A., Sabla, P. E., Seto, S. P., Taylor, J. R., and Foltz, H. P., "Energy Efficient Engine Combustion System Component Technology Development Report," NASA Final Rept., R82A EB401, Nov. 1982.